CHALMERS
UNIVERSITY OF TECHNOLOGY


# Railway ground vibration prediction using a controlled source

## Development of an empirical method predicting ground borne vibrations using a falling weight

Master's thesis in Master Program Sound and vibration

Hugo Hultén

DEPARTMENT OF SOME SUBJECT OR TECHNOLOGY

CHALMERS UNIVERSITY OF TECHNOLOGY
Gothenburg, Sweden 2024
www.chalmers.se

Master's thesis 2024

# Railway ground vibration prediction using a controlled source

Development of an empirical method predicting ground borne vibrations using a falling weight

Hugo Hultén


CHALMERS
UNIVERSITY OF TECHNOLOGY

Department of Some Subject or Technology
*Division of Division name*
Name of research group (if applicable)
Chalmers University of Technology
Gothenburg, Sweden 2024

Railway ground vibration prediction using a controlled source
Development of an empirical method predicting ground borne vibrations using a falling weight
Hugo Hultén

© Hugo Hultén, 2024.

Supervisor: Jorge Torres, Brekke & Strand Akustik
Examiner: Professor Jens Forssén, Department of Architecture and Civil Engineering

Master's Thesis 2024
Department of Architecture and Civil Engineering
Division of Applied Acoustics
Chalmers University of Technology
SE-412 96 Gothenburg
Telephone +46 31 772 1000

Cover: Picture of tram and measurement setup in Grefsen, Oslo.

Typeset in LaTeX
Printed by Chalmers Reproservice
Gothenburg, Sweden 2024

Predicting ground borne vibrations from rail vehicles –.
Development of measurement method using a controlled vibration source.
Hugo Hultén
Department of Architecture and Civil Engineering
Chalmers University of Technology

# Abstract

Rail transport today plays a major role in sustainable transportation. But ground vibrations from trains and trams create unsustainable environments that lead to irritation and affect people's sleep. Several methods are currently used to predict ground vibrations. These methods are used at different stages of railway design. Some are more accurate but costly, while others are simpler but less accurate.

In this thesis, a method for predicting ground vibrations from railways is developed. The method consists of exciting the ground with a controlled source. The controlled source used is a falling weight. The method is compared with measurements on maximum weighted vibration level for both trains and trams and for different ground conditions. To verify the measurements, a numerical analysis is also performed. Finally, a model is developed using the falling weight ground vibration measurements to model a point source or a line source of finite length. Comparisons between falling weight and rail vehicles show that the frequency spectrum differs and that the model has little resemblance with the mean value of the ground vibrations.The decay with distance of the maximum vibration level is shown to be similar to that of the rail ground vibrations when using the point source model rather than modelling a finite line source.

Keywords: Tram, Train, Ground vibration, Model, Controlled source, Falling weight, Empirical method, COMSOL.

# Acknowledgements

I would like to express my gratitude to my supervisor Jorge Torres at Brekke & Strand Akustikk that proposed the topic of this thesis. Jorge been extremely helpful throughout this project with his knowledge and assistance during measurements. In addition I would also like to express my gratitude to my supervisor and examiner Jens Forssén. Jens have supported me and his knowledge and and guidance have been instrumental in finishing this thesis. I also would like to thank Kjetil Vedholm at Brekke & Strand Akustikk that helped me with the equipment.

Finally a thanks to all the people, from students to professors, that create a wonderful environment at the Division of Applied Acoustics at Chalmers. A special thanks to Fatemeh Dashti for helping with the creation of the COMSOL model.

Hugo Hultén, Gothenburg, October 2024

# Contents

# List of Figures

# List of Tables

# 1
# Introduction

This section of the report describes the aim of the master thesis as well as giving context to the aim by providing a background to the subject. Additionally this section will include limitations to the study of what will be investigated.

## 1.1 Background

Urbanization and population growth increases the demand of transportation. Railway transportation has been around for close to two centuries and is today an important form of public transport. Today rail traffic is used both to connect cities by train and connecting the city neighborhoods by tram and subway. As of working for a sustainable future there is a broad emphasis on continuing building out the rail network [1]. Also the need for more sustainable transportation of goods will increase the amount of freight trains. An environmental issue associated with means of transportation in urban areas are vibrations. Ground-borne vibrations emitted from train traffic may cause annoyance to humans and might disturb sleep [2]. The presence of ground vibrations from trains can also potentially increases annoyance of airborne railway noise [3]. These ground vibrations are also a potential danger of interfering with sensitive equipment. Therefore predicting ground vibrations in urban areas is valuable. This is utilised when planning new railway lines and maintaining/renewing existing ones, as well as during the planning of constructing new buildings close to railways.

Today ground-borne vibrations are estimated with many different prediction models. These tools are used in all stages of the planning process and vary in cost and precision. This leads to some methods being favoured depending on the circumstances. Some methods are very time consuming while others are only useful if geotechnical and geometrical conditions can be easily described. The base for ground vibration measurements and the different methods are presented in ISO standard 14837-1 [4].

## 1.2 Aim

The aim of the thesis develop a method for predicting ground vibrations from rail vehicles. The method will predict the vibrations using a controlled source. In this thesis a falling weight will be used as the controlled source. A methodology for creating and measuring vibrations from controlled sources will be presented. The goal is to create an empirical model to predict ground vibrations from railway traffic.

To achieve the goal, the report will include and investigate the following points.

- Measurements of ground vibrations from different rail vehicles on both bedrock and soil on top of bedrock.
- Measure ground vibrations from a controlled source under the same ground conditions.
- Comparison of maximum RMS acceleration levels and frequency spectrum of vibrations from all sources.
- Comparison of the attenuation of different sources through linear regression.
- Develop a method for predicting rail vehicle ground vibrations using a controlled source.
- Creating a numerical model to compare different ground conditions.

## 1.3 Limitations

The thesis will only cover propagation of ground vibrations. It will not cover airborne sound. The model will not compare input impedance and the foundation of the track section. It will compare both the acceleration of the vibrations and the frequency spectrum. Subways and underground railway will be excluded due to time and availability constraints. The study will only cover the range 1 Hz to 80 Hz referring to the perception of ground vibration [4] , it will not include ground borne noise.

## 1.4 Specification of the issue being investigated

The prorogation of vibrations in the ground will be measured with triaxial accelerometers from both rail vehicles and a controlled source. A numerical solution will also be constructed to investigate ground attenuation of different ground conditions. The study will compare the decay of max rms levles of controlled sources and a specific rail vehicle for a certain ground condition. The comparison will be done with logarithmic regression over distance from the source. The frequency spectrum will also be compared and the end product an attempt to model the rail vehicle ground vibration with the controlled source will be made.

# 2

# Theory

This chapter will include and explain ground vibrations, how rail vehicles generate them and how different methods and models are used to predict them.

## 2.1 Ground vibration fundamentals

Vibration is at the simplest form a dynamic motion and refers to the oscillation of a point on a body around the equilibrium [5]. Shock is a term that also describes this phenomenon but refers to the event of a much shorter time period. Ground vibrations are seismic waves that includes the generation and propagation. The generation of seismic waves in combination with the ground conditions emits different kinds of propagation and in this section the main wave types of ground vibration will be discussed. The term ground vibration is broadly accepted when exclusively discussing man-made activities and disregards wave propagation from natural sources such tectonic activity [6]. It is common when describing train induced ground vibration to talk about the source, the propagation and the receiving structure. In this thesis the main focus is the propagation.

### 2.1.1 Generation

Vibrations from rail vehicles are produced mostly the same way air borne sound from rail vehicles are created. It starts with the train, the cars of the train and the engine, exiting the track which then transmit the energy into the ground. Important factors in this system are the wheels and axles. The vibrations are dependent on the axial load, the configuration of the wheels on the train, and wheels connection to the bogie and rest of the body [7]. The weight in the car body is transferred to the rail thought the bogie and suspensions as see in figure 3.3 The velocity and the acceleration of the train are also big contributing factors. When examining the generation of ground vibrations it is of importance to recognise the large differences for similar conditions. This is caused by the stochastic nature of ground vibrations from trains where small changes can lead to drastically different outcomes. The full extent of of the generation process is still being researched but it is agreed that there are two main components that drive the ground vibrations. The generation can be classified into the categories, dynamic load and quasi static, also referred to as moving load.

#### 2.1.1.1 Dynamic loads

Rolling noise and ground vibrations have the same source mostly due to dynamic loads. This occurs when irregularities on the wheel and track leads to displacements that causes a periodic force. Irregularities on surface between the wheel and the track can be referred to as roughness [8]. This displacement is a time dependent deformation that aligns with the wheel frequency. The irregularities on the wheel are caused by extensive breaking but things such as rail joints and switches on the track also generate dynamic forces. The difference from the generation of rolling noise and ground vibration is that longer wavelengths of roughness are involved with ground vibration [8]. The change in ground conditions and the change in stiffens due to passing of sleepers can create parametric excitation.

#### 2.1.1.2 Quasi static load

Moving load or the 'quasi-static excitation' mechanism occurs when the weight of the train transmitted through the wheel causes a local deflection on the track[8]. This vertical deformation persists along the track as the train runs along it. Moving loads are only present in the near-field for vehicle speeds of trains operated in commuting traffic in relative low speeds. Nevertheless, buildings close to the track might still be affected, due to the relatively long wavelengths of these low frequency vibrations. For example, for a standard wheelbase it is shown that the contribution from a moving load is dominant up to 25 Hz at a vehicle speed of 100 km/h [8].

#### 2.1.1.3 Source

It is not easily determined where the source of the ground vibrations is located. Except for the wheels and the rail, the track embankment can differ considerably. Source contribution and the source mechanism that excite ground at different frequencies is important when understanding and predicting ground vibrations. Wheel passing over the rail joint have been studied as main contributor [9]. Here it is shown that the frequency spectrum of the ground vibrations are heavily influenced by the axle passing frequency and its overtones. Other examples have investigated how the sleepers could be the substantial factor. Due to the quasi-static deflection at each sleeper generating ground vibration the vibration spectra is therefore highly influenced on the axial loading [10].

### 2.1.2 Propagation

#### 2.1.2.1 Types of wave movement

Seismic waves can be classified into two different main type of waves, body waves and surface waves. Body waves or volume waves are categorized into two type of waves, primary/pressure waves (P-waves) and secondary/sheer waves (S-waves) [5]. P-waves are a longitudinal waves that compresses the body parallel to the propagation. S-waves are transversal waves that shear the body transversal to the propagation. Body waves propagate in all directions[5].

Surface waves consists of many different type of waves but the most important one for train induced ground vibration is the Rayleigh waves (R-wave). Surface waves such as Rayleigh waves develops at the at the boundaries of two materials with drastically different impedance, like at the ground surface between soil and air. As the name implies, surface waves propagate along the surface and the amplitude decreases abruptly in vertical direction. For Rayleigh waves the particle motion is backward elliptical in the direction of the propagation [5]. Love waves (L-wave) is also a surface wave but is often disregarded in the context of man made ground vibration.

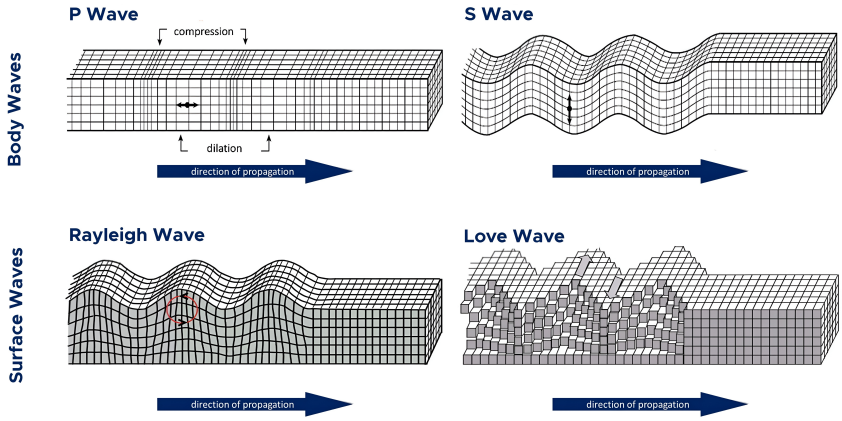


**Figure 2.1:** Different wave propagation in ground. [11] [12] [13]

### 2.1.3 Propagation properties

Propagation mechanisms for ground waves can be categorized into either shearing or compression. It is also possible for a combination of both mechanisms. These two mechanism presents two fundamental wave speeds that are calculated by Eq (2.1), where $c_1$ is in the speed of compression waves and $c_2$ the speed of shear waves.

$$c_1 = \sqrt{\frac{\lambda + 2\mu}{\rho}}; \quad c_2 = \sqrt{\frac{\mu}{\rho}} \tag{2.1}$$

The formula also states that compression waves are faster. The variables $\lambda$ and $\mu$ in the are know as the Lamé constants and describes the material properties. Lamé constants are defined by Eq (2.2)

$$\lambda = \frac{\nu E}{(1+\nu)(1-2\nu)}; \quad \mu = \frac{E}{2(1+\nu)} \tag{2.2}$$

This means that when soil is simplified to a solid elastic material, the two defining factors of wave speed are Young's modulus, $E$ and Poission's ratio $\mu$. Rayleigh waves propagate with a combination of shear and compression mechanism. Rayleigh waves propagates with a slower velocity than the body waves. Depending on the soil, the speed is about 90% of the shear wave speed and contrary to compression wave speed, it is not frequency dependant [14]. If a source excites the ground with the same speed as the Rayleigh waves, radiation impedance decreases and a small exaltation amplitude could lead to large displacement. The speed of ground waves

are slower in soft soil, that means that Rayleigh waves in soft soil is a often critical speed when planning new railways. This is usually only a problem for high speed railway. In figure 2.2 the speed for ground waves for different Poisson raito are presented normalized to the S-wave speed.

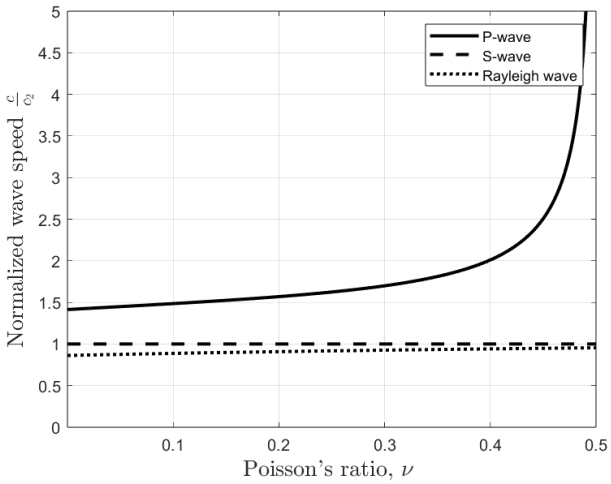


**Figure 2.2:** Ground vibration wave speed normalized to the S-wave speed.

The wave type generated by the train is depended on the size of area excited in relation to the shear wavelength. If the area is large compared to the wavelength most of the energy is transmitted as body waves. The other scenario where the area is small leads to most of the energy being carried as surface waves[14].
When the ground can't be modeled homogeneous due to the vertical ground layers. It is often proposed to use analytical or numerical models to model propagation [15]. The ground not being homogeneous also emphasises the severity of the contribution of body waves. Even if body waves propagate deep into the ground the propagation of wavefront diffract, reflect and refract due to natural condition of the soil.

### 2.1.4 Reflection and refraction

To further understand the differences of ground vibrations depending on the soil a few mechanism related to soil will be presented reflection and refraction. When a ground wave traveling through a medium encounters a layer with different material properties, different impedance, refraction and reflection of the wave occurs. Refraction and reflection can cause interference patterns that amplify or cancel out certain frequencies.

## 2.2 Damping

Vibrations wave energy that travel through the ground will decay as it propagates away from the source. There are two dampening mechanism that attenuate ground vibrations.

### 2.2.1 Geometrical attenuation

Geometrical attenuation in ground vibrations refers to Lambs mathematical solution to how body and surface waves attenuate in an elastic half-space. In equation 2.3 the peak velocity $\hat{v}$ at distance $r$ is related to the peak velocity $\hat{v}_1$ at the distance $r_1$ dependingon the propagation, the source type, and the wave type that corresponds to the coefficient $m$ as seen in table 2.1.

$$\hat{v} = \hat{v}_1 \left( \frac{r_1}{r} \right)^m, \tag{2.3}$$

**Table 2.1:** Wave propagation characteristics [16]

| **Propagation** | **Source type** | **Wave type** | $m$ | **Decay factor** |
|---|---|---|---|---|
| Along surface | Point source | Body wave | 2 | $\frac{1}{r^2}$ |
| Along surface | Point source | Surface wave | 0.5 | $\frac{1}{\sqrt{r}}$ |
| In half space | Point source | Body wave | 1 | $\frac{1}{r}$ |
| Along surface | Line source | Body wave | 1 | $\frac{1}{r}$ |
| Along surface | Line source | Surface wave | 0 | No decay |
| In half space | Line source | Body wave | 0.5 | $\frac{1}{\sqrt{r}}$ |

### 2.2.2 Material damping

The other factor of ground wave attenuation is material damping. This loss of energy is caused by friction in the material. Stiffness of the ground determines the damping. Stiffer soil and bedrock have the lowest damping. The amount of attenuation not only depends on the ground condition but also the vibration amplitude and the frequency [17].

## 2.3 Near-field

When observing ground vibrations caused by rail vehicles a near-field and far-field can be exhibited. A general definition of the terms is that the far-field begins a distance r away from the source where the vast majority of the vibration energy is propagated as Rayleigh waves, as described by Gao et. al [18]. Closer to the source other wave types such as P- and S-waves contribute to the ground vibration. Determining where the near-field ends and the far-field begins is not a straight forward problem. The boundary between them have been discussed plenty throughout the years but were mostly investigated looking at a point source. The location of the boundary changes with many parameters like the source and the stiffness of the ground [18]. Gao present a solution by looking at lambs problem [19] for a harmonic and infinite line source at the surface of a geometrical half space. The determination of the boundary from a point source is about 5 to 6 times the wavelength in stiff ground and around 2 to 3 times the wavelength in soft soil. This boundary is increased slightly for the scenario with an infinite line source. A simplified observation concludes that body waves are influential up to 20 meters from the source [20].

It is also noticed that material damping has a minor effect on vibrations near the source, but significantly impacts vibrations further away. This indicates that the attenuation of vibrations close to the source is primarily caused by geometric damping, while material damping becomes more influential at greater distances from the source. The waves attenuate more rapid for a point load, and it is also noted that boundary is predicted further from the source is material damping is ignored.

## 2.4 Prediction models

To predict ground vibrations from rail vehicles a number of methods for models can be used. The models can both be based on mathematical theory or be experimental. A model should include vibration magnitude at different distances from the source. For a thorough model the impact force, the damping and propagation as well as the transmission into building should be considered. The three main models of predicting vibrations are presented below.
The different model also have different requirements though out the planning process described in ISO 14837-1 [4]. Usually this process only should be used for prediction levels of a new railway, whereas modifications to old ones should be compared to previous assessments. The different requirements can be inserted into three stages of prediction accuracy.

- **Scoping model**: This model is the least complex model. The purpose is to make a rough "worst case" prediction of the overall levels in the beginning of the planning process. Only the most basic parameters should be used such as: vehicle type, distance to receiver, basic description of ground conditions and how sensitive the receiver is to disturbance. The aim is to find at what distance, from the center of the rail system, the levels of ground vibrations are very unlikely to cause disturbance.
- **Environmental assessment model**: The next step after the scoping model is to more accurately describe the location and also include solutions to mitigate the vibrations. The environmental assessment model includes more parameters and includes, as an example, the supporting structures of the track and how the track is aligned vertically and horizontally. Another importance aspect of the requirements for this model is that the frequency content of the vibration needs consideration.
- **Detailed design model**: Detailed design model is used both to predict absolute values or just predict change in levels considering a specific aspect of ground vibrations. When considering a certain aspect, like the source, that output could be an input to an Environmental assessment model. For this model vibrations needs to be described by the frequency content in either narrow band, octaves or one-third-octave bands.

### 2.4.1 Empirical method

Empirical models rely on experimental data and predict data relationships based on empirical observations. In project planning it can be used at an early stage. A semi-empirical model, class one, was created based on train measurements in

Sweden by Bahrekazemi [20]. A total of four measurements sites with different ground conditions are investigated. The trains considered are both fright trains and passenger trains operating at normal traffic conditions. The model aims to correlate particle velocity in close proximity to the track with the speed of the train and the wheel force. A linear relation between the rms-value of particle velocity and wheel force is then set seen in equation 2.4.

$$V_{\text{rms}} = a \cdot \text{speed} + b \tag{2.4}$$

The variables a and b depend on both site conditions and the wheel force. The model uses the propagation to the close proximity reference distance to calculate the attenuated vibrations further away. Lastly the model is integrated in a Geographical Information System, GIS, to get a comprehensible overview of the environment vibrations. Bahrekazemi [20] also creates a second model, class two, as an improved version of the first one. The ground vibrations are now considered as several subsystems that can be studied individually. The subsystems consist of the track, near-field influence, transfer path and the receiving building. The transfer path is modeled as superposition's of multiple waves. It focuses on compensating for the non linearity and character of the event.
Another semi-empirical model is described by Madshus et al [21]. The model was developed in Norway when projecting and building a new high speed railway. It is founded upon measurements done in both Norway and Sweden that both have similar ground conditions with soft soil of post glacial clay and silt deposits. The model focuses on the low frequency vibration at 5-10 Hz and 30-50 Hz that are even more prominent in soft soils. The model sums up all the contributing factors in to three variables Eq (2.5).

$$V = F_V F_R F_B = [V_T F_S F_D] F_R F_B, \tag{2.5}$$

$F_V$ describes the vibration function and $F_R$ and $F_B$ covers the condition of the track and the response from the building respectively. The vibration function $F_V$ is made up of distance and speed factors, $F_D$ and $F_S$, and the vehicle specific vibration level $V_T$.

### 2.4.2 Numerical method

Ground vibrations can be approximated by finding the solution through convergence of mathematical equations using computational power. These numerical methods excels in soil wave propagation over analytical methods where the the excitation needs to be stationary as well as other simplifying assumptions.
The finite element method (FEM) is a numerical method that uses a weak form of the seismic wave equation. It is effective at describing the propagating around the track structure and in the near-field [**?**]. A problem with FEM calculations is that it can be cumbersome. Other methods are just not as tedious and the amount of work that has to be put into FEM might not justified when considering the a quicker, marginal better solution. A reduction in computation time is possible by solving it in the frequency domain rather than the time domain. This solution is also not straight forward since describing the boundary conditions as non reflecting is

challenging to put into practices in the frequency domain. FEM can be analyzed in both 2D and 3D. By looking in only two dimensions, computations times are reduced greatly but the information of the propagation along the track is lost. Studies in 3D-modeling have been carried out with varying success[22] [23].
FEM can also be interpolated with the boundary element method (BEM). This has the advantage of calculating ground vibration further from the source.

### 2.4.3 Analytical method

The analytical methods, based on mathematical equations, for predicting ground vibrations are preferred because of their efficiency in time and cost. However they can lack in accuracy due to oversimplification. To model a rail the most simple variation is using an Euler Beam. This have been proven to lead to a low accuracy for a large range of frequencies [24]. Even with more advanced methods, like accounting for the shear deflection and the rails resisting of rotation still did not see any improvements at the relevant frequencies for ground vibrations.
In addition to the analytical model there have also been attempts at calculating the transfer functions using a falling weight. Examples of this have been measuring the response of the ground by dropping heavy steel ball used in shot putting [9].

# 3

# Methodology

To investigate ground vibrations, in-situ measurements were carried out in the rail and tram network Oslo, Norway. These measurements also included ground vibration generated through a controlled excitation by a falling weight. The measurements were carried out at 4 different locations in Oslo. Two of these locations were used to investigate the ground vibrations from trams, while the other two locations exhibited ground vibrations from passenger trains. The measurement took place on 1 May 2024 and 2 May 2024. The temperature was not recorded, however it was of importance that the ground was not frozen and the temperature was well above the freezing point. The first part of this section will cover the details of the measurement setup and the specifications of the measurements locations. A numerical model was build in Comsol and its predictions compared to the measurements data.The characteristics of this model are further discussed in the second part of this chapter

## 3.1 Measurement setup

Measuring ground vibrations from rail vehicles requires multiple sensors to capture the induced ground vibrations. This was done by placing and connecting multiple accelerometers at different distances from train and trams tracks. This recorded the particle acceleration in the ground for each tram/train passing. With the same set up for measuring the rail vehicles a second measurement was conducted. Instead of measuring the rail vehicles a falling weight was used to excite the ground.

The measurement setup was the same for all locations, except for a slight deviation for the measurements at Nordstrand which will be discussed later. The measurement used 6 tri-axial accelerometers. The accelerometers were positioned in a straight line perpendicular to the track. The full set up and the distances can be viewed in figure 3.1. To assure that the sensors were stable, the sensors where placed on top of a metal foundation shown in figure 3.2. The foundation were placed in the ground and leveled with a spirit-level.

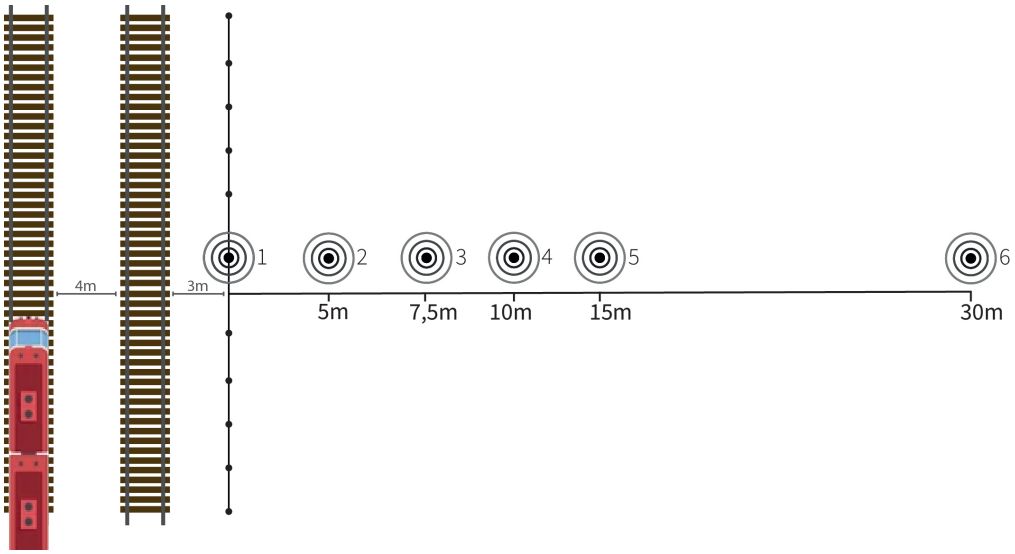


**Figure 3.1:** Positions of the sensor in the measurement set up.

The first sensor was placed as close to the track rail as possible, 5 meters from the center line of the track section. From that point a measuring tape was used to place the remanding sensors in a perpendicular line away from the track. The distances were selected with the logarithmic behaviour of vibration propagation in mind.


**Figure 3.2:** Sensor, mounted on top of a metal foundation at Grefsen.

### 3.1.1 Rail vehicle

At each measurement site 5-8 vehicles pass-by were recorded. Standards for measuring vibration levels for comfort is 15 vehicles per site [25]. Since these measurements are not considering comfort levels or propagation into buildings a lesser amount of recordings was deemed sufficient. Each passing was filmed with a camera connected to the recording equipment. The time of the pass by was also recorded with a stopwatch to calculate the speed of the vehicle. Every location investigated had double track system. The last step for each measurement was to note the model of the train and in which direction the train passed.

### 3.1.2 Controlled excitation

The second measurement consisted of dropping a falling weight. The excitation point of the controlled method was the same, or as close as possible, to the location of the first sensor. For the falling weight a 48 kg kettle bell was used. To consistently excite the ground the weight was hoisted on a ladder with markings for 0.5 m, 0.8 m, and 1 m. The contraption used is shown in figure 3.11. The weight was dropped three times for each height at each location.

### 3.1.3 Equipment

To record ground vibrations there needs to be a transducer that responds to the oscillation in the ground and a data acquisition system that digitises and stores the data. In this study tri-axial accelerometers were used together with two connected Head acoustics SQadrigas. The accelerometers used where PCB tri-axial accelerometer Model 356B18. These accelormeters record in three directions for each sensor set up to measure acceleration vertical, perpendicular and parallel to the rail. The accelrometers used are piezoelectric and create a change signal. That signal is transformed into a voltage signal that is then transmitted through a general purpose output cable. The accelerometers used have a sensitivity of 102 $\mathrm{mV/(m/s^2)}$, and a frequency range between 0.5 Hz and 3000 Hz. For the SQuadrigas, both a model 2 and a model 3 where connected to each other making a total of 16 channels available. Since there were 6 sensors with three directions, 18 would have been needed to record every direction. This led to the decision to not include the y-direction, which is perpendicular to the rail, to be not included for the first and forth sensors.

The accelerometers where calibrated before the measurements using a vibration calibrator PCE-VC21. The full accelerometer calibration data sheet is presented in table 3.1.

**Table 3.1:** Accelerometer Data Table at 100 Hz

| ID | Serial No. | Date | X | Y | Z | Unit |
|---|---|---|---|---|---|---|
| **VIK-ACC01** | LW204334 | 06.03.2024 | 105.90 | 100.54 | 102.27 | $mV/ms^2$ |
| **VIK-ACC02** | LW309220 | 06.03.2024 | 102.61 | 101.48 | 101.63 | $mV/ms^2$ |
| **VIK-ACC03** | LW204335 | 07.03.2024 | 104.03 | 105.10 | 103.57 | $mV/ms^2$ |
| **VIK-ACC04** | LW204068 | 08.03.2024 | 99.21 | 107.37 | 101.84 | $mV/ms^2$ |
| **VIK-ACC05** | LW200845 | 07.03.2024 | 102.98 | 103.92 | 105.09 | $mV/ms^2$ |
| **VIK-ACC06** | LW204467 | 08.03.2024 | 107.51 | 103.81 | 102.37 | $mV/ms^2$ |

## 3.2 Location description

As stated earlier the measurements was done at 4 locations. The locations were picked by looking at a satellite and geological data along the tram and train tracks in Oslo. The aim of the locations investigated was to find a site with only bedrock and a site with a layer of soil on top of the bedrock for each vehicle type. Through google maps the locations were verified so that it was enough space, relatively flat and without buildings. The ground conditions was investigated using data from NGU, Norges Geologiske Undersøkelse. The maps used to choose the locations where maps of soil layer and bore hole, depth to rock [26] [27]. Since no drilling or other investigations were carried out, the soil map and previous bore holes are the only information available and is a rough estimation of the actual ground conditions.

Table 3.2 presents all the locations investigated and ground conditions that have been assumed. The ground condition is based on the closest borehole available at NGU [26].

**Table 3.2:** Recording Details Table

| **Location** | **Vehicle Type** | **Ground Condition** |
|---|---|---|
| Grefsen | Tram | 6.5 m Clay on top of bedrock |
| Nordstrand | Tram | Bedrock |
| Bryn | Train | Bedrock |
| Lysåker | Train | 5 m Filling mass on top of bedrock |

### 3.2.1 Measurements at Grefsen

This location was picked to investigate vibrations from tram with clay on top of bedrock. At Grefsen the measurement was done on five trams. Three of the trams were on the closer track and two were on the further track. This was the first location and it was also where the range was changed to avoid overload. The first sensor was located in a flowerbed where the topsoil had been changed. Between the first and the second sensor was a paved bike and walkway. The set up can be seen in figure 3.3 and the location in figure 3.4.

**Figure 3.3:** Measurement Setup for Grefsen

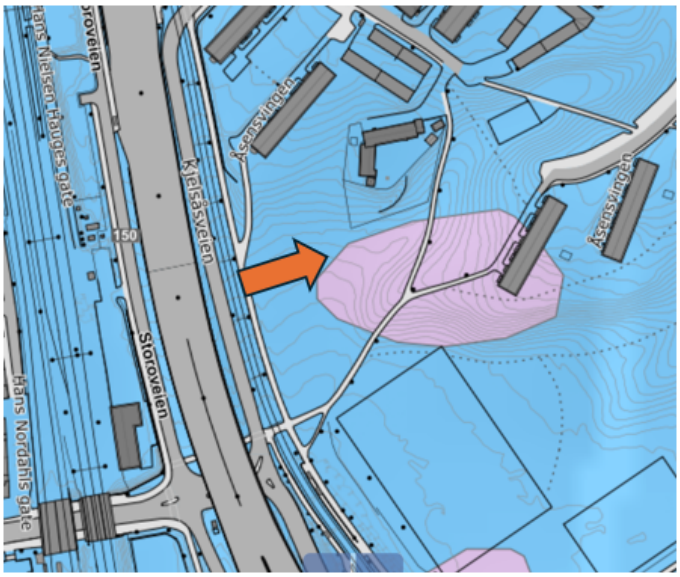


**Figure 3.4:** Ngu geological map, location and direction of the set up marked with a orange arrow [27].

### 3.2.2 Measurements at Nordstrand

This location investigated vibrations from trams on bedrock with little to no soil on top. At Nordstrand 8 trams were recorded with four pass-by each at the closer and

outside rail. At this location it was only possible to measure up to 15 meters from the rail and only the first 5 sensors were used. On the opposite side of the track section there was a building site but this was not picked up by the accelerometers. No other disturbances were noted. The set up can be seen in figure 3.5 and the location in figure 3.6.

**Figure 3.5:** Measurement Setup for Nordstrand


**Figure 3.6:** Ngu geological map, location and direction of the set up marked with a orange arrow [27].

### 3.2.3 Measurements at Bryn

At Bryn the vibrations from train on bedrock was investigated. 5 recordings were done. Two of the recording were unfortunately corrupted due a problem with the

video recording. For the three recording 2 were on the track furthest away and one closer. As with Grefsen a paved walkway crossed the between the first and the second sensor. There was also just barley enough space to place the sixth sensor furthest away. The last sensor ended up in a slope about half a meter below the elevation of the other sensors. The set up can be seen in figure 3.7 and the location in figure 3.8.

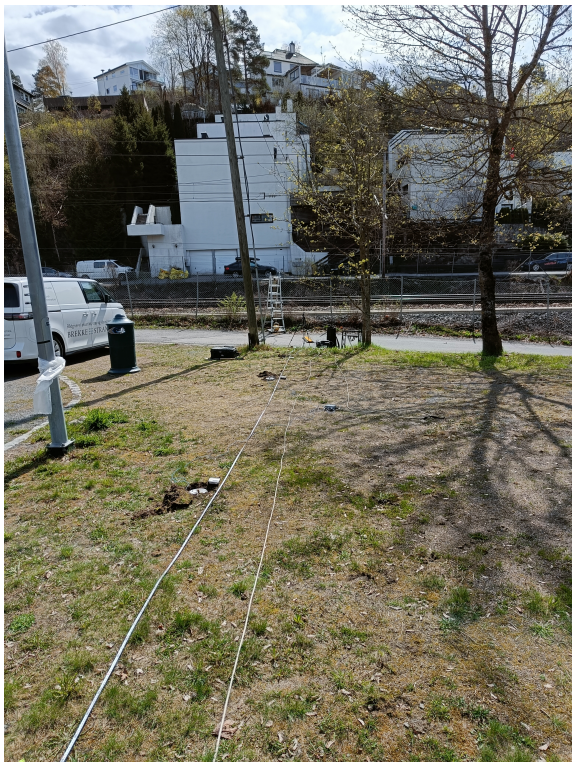

**Figure 3.7:** Measurement Setup for Bryn

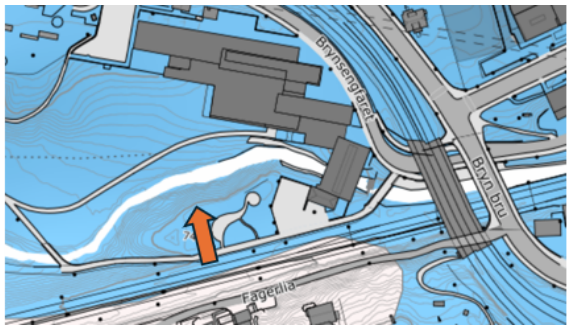


**Figure 3.8:** Ngu geological map, location and direction of the set up marked with a orange arrow [27].

### 3.2.4 Measurements at Lysåker

At Lysåker ground vibrations from trains where measured. The purpose was to investigate the ground condition soil on top of bedrock. Unfortunately a location with this condition was hard to find. The ground condition at Lysåker was filling

mass on top of bedrock.

**Figure 3.9:** Measurement Setup for Lysåker


**Figure 3.10:** Ngu geological map, location and direction of the set up marked with a orange arrow [27].

## 3.3 Vehicle types

There were different vehicles and vehicle model measured at each site. Most of the specific individual vehicles were recorded with the camera but it will not be investi-

gated further in this report. It is assumed at most measurements a different specific vehicle was recorded. Table 3.3 presents the two tram models that where measured. In table 3.4 the two train models are described. For the tram measurements, the models were different at the two locations. For the train measurements, the train Type 72 model was measured at both Bryn and Lysåker while the Type 69 model was only measured at Lysåker. The Type 69 train can be found with both two and three cars and the cars also change slightly trough out the manufacturing years. In this study only three car trains were measured and it is for that type the numbers below represent.

**Table 3.3:** Tram Vehicle Specifications

| **Location** | **Grefsen** | **Nordstrand** |
|---|---|---|
| **Name** | SL18 | SL95 |
| **Manufacturer** | CAF | Ansaldo/Firema |
| **Length** | 34.2 m | 33.1 m |
| **Weight** | 42 700 kg | 64 000 kg |
| **Track gauge** | 1,435 mm (standard gauge) | 1,435 mm (standard gauge) |
| **UIC classification** | Bo'+2'+Bo' | Bo'+Bo'+Bo' |


**Figure 3.11:** SL18 tram at Grefsen with the falling weight setp up.

**Table 3.4:** Train Vehicle Specifications

| **Location** | **Bryn/Lysåker** | **Lysåker** |
|---|---|---|
| **Name** | Type 72 | Type 69 |
| **Manufacturer** | AnsaldoBreda | Strømmens Værksted |
| **Length** | 85.7 m | 73.5 m |
| **Weight** | 164 000 kg | 120 000 kg |
| **Track gauge** | 1,435 mm (standard gauge) | 1,435 mm (standard gauge) |
| **UIC classification** | Bo' 2' 2' 2' Bo' | Bo'Bo'+2'2'+2'2' |

## 3.4 Data processing

The acceleration data in time domain was available as HDF-files and converted to wav-files. The data was then processed in MATLAB. The data that was recorded was acceleration data in $\mathrm{m/s^2}$ in one of the three dimensions. The data was then processed in alignment to the guidelines for environmental quality reference value [28]. The reference value is of maximum $14\,\mathrm{mm^2}$ and is calculated as by the standard of human response to vibration [29] and is a weighted maximum root mean square value (max rms). The max rms, $a_{w,\theta}(t)$, is the one value maximum acceleration of all directions when averaging over a specified time. All rms values compared in this thesis are weighted values.

The signals were first filtered into third octave bands from 1 Hz to 80 Hz. Each third octave band was weighted according to whole body frequency weighting $W_\mathrm{m}$, used for whole body vibration considering all directions. The weighting $W_\mathrm{m}$ is presented in appendix A.1. The signal was then added back together creating a weighted time signal. The running rms acceleration value, $a_{w,\theta}(t)$ was then calculated like (3.1).

$$a_{\mathrm{w},\theta}(t) = \left(\frac{1}{\theta}\int_{t-\theta}^{t} a_\mathrm{w}^2(\xi)\,d\xi\right)^{1/2} \tag{3.1}$$

This was done using the movmean() function in matlab with the integration time $\theta$ of 1 second. $a_\mathrm{w}(\xi)$ is the weighted acceleration at time ($\xi$).

$$L_\mathrm{w} = 20\ \lg\left(\frac{a_{\mathrm{w},\theta}(t)}{a_0}\right)\ \mathrm{dB} \tag{3.2}$$

The acceleration is then converted to levels, $L_\mathrm{w}$ using equation (3.2) with the reference value $a_0 = 10^{-6}\,\mathrm{m/s^2}$. $L_\mathrm{w}$ is the time-averaged weighted acceleration level.

To compare the decay in the measurements of the trains and trams to the controlled excitation linear regression model was used. Here the decay in the near field was investigated. That excluded the data from the closest sensor to the controlled excitation. In the near field the tram will be assumed to be a line source and the controlled excitation a point source. It is expected that the ground vibrations from these sources to decay logarithmic a logaritmic fit was done using using the function logfit that used the command polyfit() in matlab.

The last step is creating the model. The model is made by placing many point sources along rail, the length of the rail vehicle. The point sources represents the axial loading of the wheels. The point sources are based on the decay of the falling weight. The sources are added together assuming uncorrelated sources using equation (3.3) for addition of uncorrelated sources. Assuming the vehicles center being aligned with the sensors, $L_{w,1}$ ,$L_{w,2}$ and $L_{w,\ldots}$ is the levels of the falling weight at the distance corresponding to a straight line between a point on the vehicle and the sensor.

$$L_{\mathrm{w,tot}} = 10\log\left(10^{L_{\mathrm{w},1}/10} + 10^{L_{\mathrm{w},2}/10}\right) \tag{3.3}$$

## 3.5 Numerical method

To investigate further on ground vibrations from a point source a 3D finite element method model was done in COMSOL. The method was done to understand the different ground response of a layer of soil on top of bedrock compared to just bedrock. Two ground models were made, one with only bedrock and one with a layer of soil on top of the bedrock. The conditions in the two models were crated based on the conditions at Grefsen and Nordstrand.
The model assumes linear elastic properties and low reflecting boundary conditions to agree with the continuous propagation in the ground by avoiding undesirable reflections that a finite geometry creates.
The mesh size on the models were created by calculating the critical wave speed using equation (2.1) to calculate shear wave speed and estimating the Rayleigh wave speed.

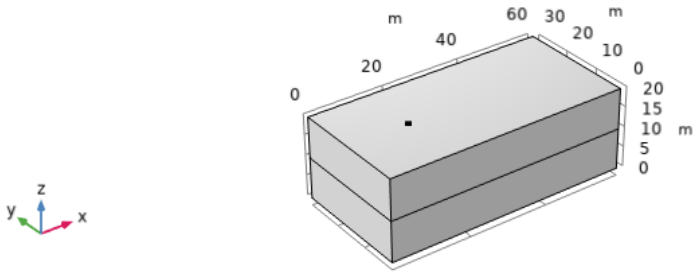


**Figure 3.12:** Linear regression for all by passes and the average regression of the falling weight.

# 4

# Results

The results from the measurements and the Comsol model are presented here. The result will include an analyze of the soil particle acceleration and the frequency content of the ground waves. The excitation from the rail vehicles will be compared to the falling weight excitation at each combination of ground condition and vehicle type. This will include a linear regression analysis of the propagation decay and compare it to know attenuation of line and point sources.

## 4.1 Acceleration level

This section will cover the ground particle acceleration from the measurements. Acceleration levels $L_{\mathrm{w}}$ are presented for each vehicle and each controlled source excitation. The results are presented on a logarithmic x-axle. For each location every passage and controlled excitation is given. The reference value for human disturbance from railways is included.

At he first measuring site, Grefsen, vibration data is presented in figure 4.1. For the trams a large range of vibration energy is observed with over 10 dB differences between individual vehicles. The highest level can be observed for the closest measurement position and is 90 dB. The acceleration level is of similar magnitude between 5 m and 10 m from the source. For two trams the acceleration level is still above the reference value for human disturbance. The decay of the vibration is much more rapid between around 10 meters to 20 meters. The falling weight measurements provide equal magnitude as the trams. At 7.5 m the highest maximum acceleration for any tram and the controlled source matched. At most positions the ground vibration level from the controlled source were in between the tram with the highest level and the tram with the lowest level. The acceleration level at 5 m for the falling weight with most energy were around 84 dB.

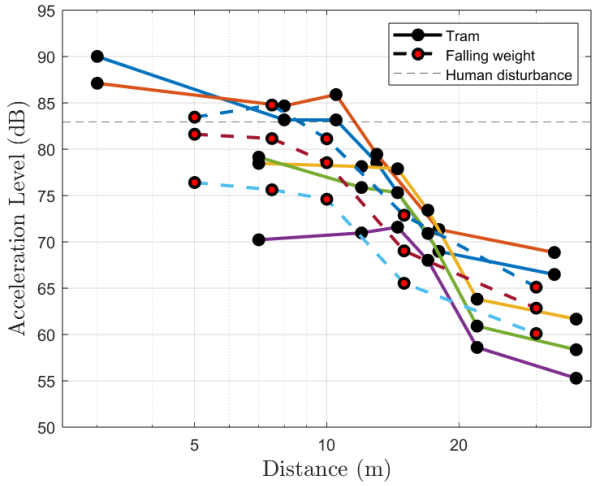


**Figure 4.1:** Acceleration levels of both rail vehicles and falling weights at Grefsen.

The acceleration levels at Nordstrand are presented in figure 4.2. The ground vibration at Nordstrand was only measured with five sensors. The sensor furthest away was 15 m from the controlled source excitation. At no sensor is the ground vibration exceeding the disturbance reference value. There was a clear difference in levels between the trams going in the opposite directions with. The trams on the nearest track have higher levels except at around 12 m. For some trams the penultimate measurement position have a higher acceleration level then the last one. The acceleration level declines faster for the falling weight than for the trams between 5 m to 10 m. At 10 m the ground vibrations from the trams decay faster. The acceleration level at 5 m for the falling weight with most energy were around 84 dB.

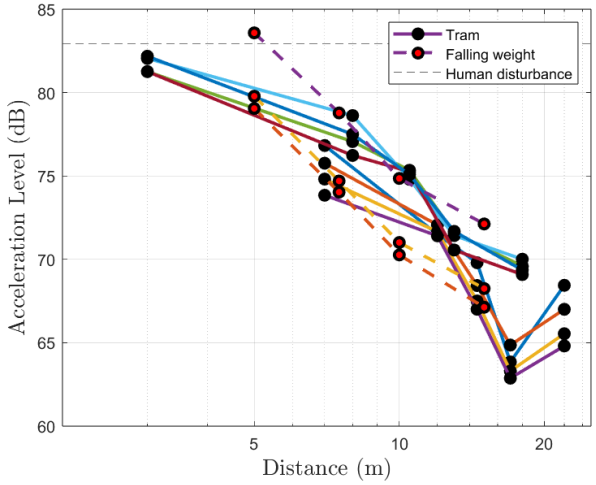


**Figure 4.2:** Acceleration levels of both rail vehicles and falling weights at Nordstrand.

The acceleration levels at Bryn are presented in figure 4.3. The acceleration levels were high close to the source, well over the reference value for on tram. There were a

steady decay until 15 m for both trams and the falling weight. For all measurements, the penultimate measurement position have a higher acceleration level then the last one. The acceleration level at 5 m for the falling weight with most energy were around 94 dB.

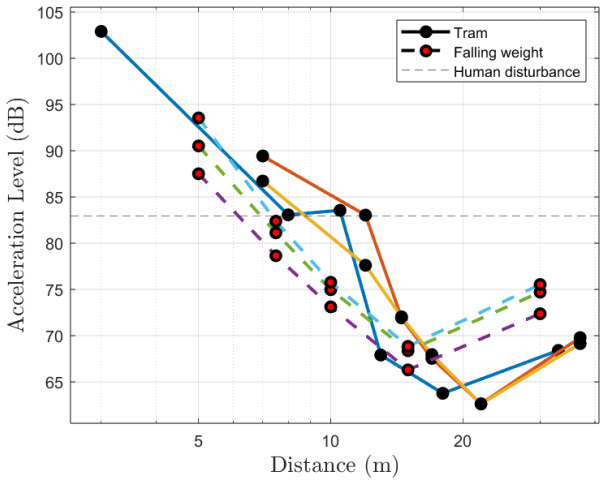


**Figure 4.3:** Acceleration levels of both rail vehicles and falling weights at Bryn

The acceleration levels at Lysåker are presented in figure 4.4. For the trains a large range of vibration energy is observed with over 10 dB differences between individual vehicles. There is a steady decline in acceleration level for the trains at all measurement positions. The acceleration level at 5 m for the falling weight with most energy were around 93 dB. The acceleration level were high in compared to the trains closer than 10 m from the source. After 10 m the falling weight decrease a lot.

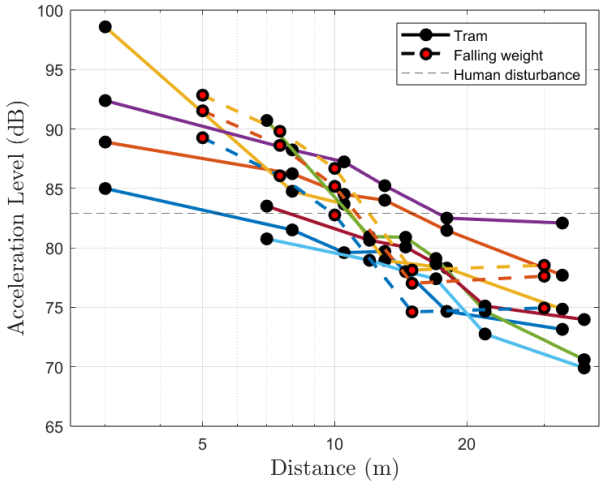


**Figure 4.4:** Acceleration levels of both rail vehicles and falling weights at Lysåker.

To compare the influence of speed on the vibration level two examples are provided in figure 4.5 and 4.6. Here the speed of the individual trams are shown as well as the

vibration level. At Grefsen, see figure 4.5 the trams had a large difference in level between individual vehicles. The trams had similar speed with the slowest tram having the highest acceleration level. At Nordstrand, see figure 4.6 the trams had a small difference in level between individual vehicles. The trams had similar speeds with the fastest tram having the lowest acceleration levels.

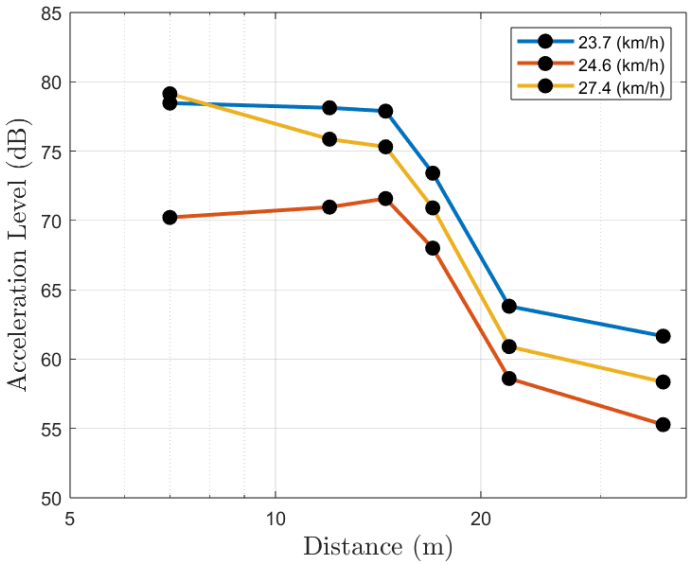


**Figure 4.5:** Acceleration levels of rail vehicles at different speed at Grefsen.

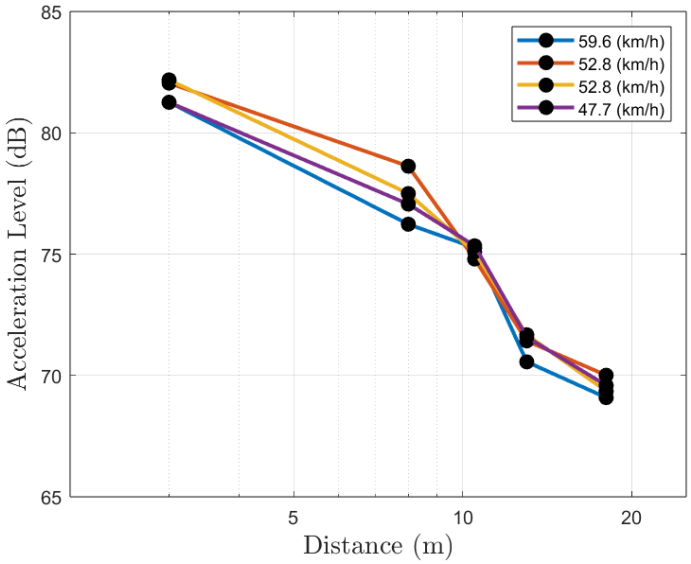


**Figure 4.6:** Acceleration levels of rail vehicles at different speed at Nordstrand.

## 4.2 Spectrum

The frequency spectrum will be presented for two vehicles passages, one in each direction of the track, and the falling weight at with the most energy. The distance investigated will be at around 10 meters at every location. The frequency spectrum's compared are of the signal in the vertical direction. The spectrum is in third octave bands, and is also weighted according to human disturbance $W_{\mathrm{m}}$. The narrow band spectrum at each location is presented in appendix A.1 A.2 A.3 A.4.

In figure 4.7 the spectrum for Grefsen is shown. The falling weight exhibits a significant lower level at low frequencies below 10 Hz than the vibrations from the trams, but exceeds them above 10 Hz. The maximum vibration level for the tram is around 5 Hz and around 85 dB for the position at 8 m and around 80 dB for the position at 12 m. The maximum level of the falling weight is around 85 dB at around 50 Hz. In figure 4.8 the spectrum in third octave bands is weighted. The maximum level of the tram vibration is 65 dB at 1 Hz for the position of 8 m and 60 dB at 5 Hz for the position at 12 m, while the falling weight induces a vibration level of 35 dB at 10 Hz. The slightly higher level of the falling weight compared to the tram can be see above 20 Hz but is much lower than the maximum vibration level at 10 Hz.

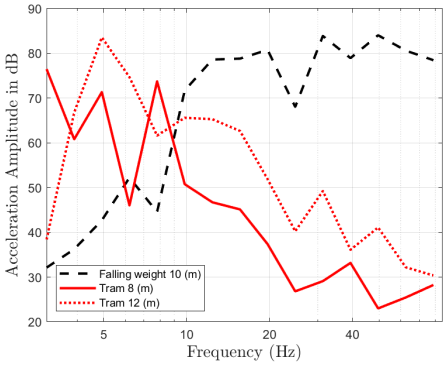


**Figure 4.7:** Frequency spectrum at Grefsen in third octave bands.

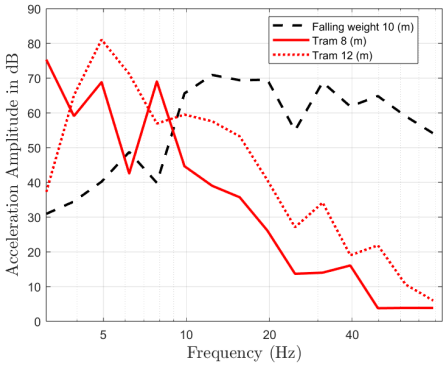


**Figure 4.8:** Weighted spectrum, third octave bands, Grefsen.

In figure 4.9 the spectrum for Nordstrand is shown. The falling weight exhibits very significant lower level at low frequencies below 10 Hz than the vibrations from the trams, but is similar above 10 Hz. The maximum vibration level for the tram is around 10 Hz and around 85 dB for the position at 8 m and around 75 dB for the position at 12 m. The maximum level of the falling weight is around 70 dB at around 20 Hz. In figure 4.10 the spectrum in third octave bands is weighted. The maximum level of the tram vibration is 80 dB at 10 Hz for the position of 8 m and 70 dB at 7 Hz for the position at 12 m, while the falling weight induces a vibration level of 60 dB at 20 Hz. A similar level of the falling weight compared to the tram can be see above 20 Hz but is much lower than the maximum vibration level at 10 Hz.

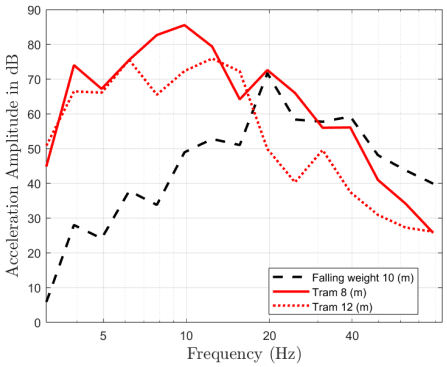


**Figure 4.9:** Frequency spectrum at Nordstrand in third octave bands.

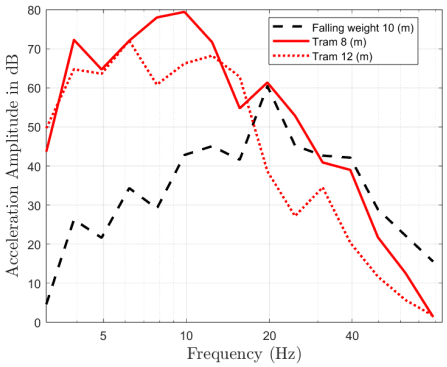


**Figure 4.10:** Weighted spectrum, third octave bands, Nordstrand.

In figure 4.11 the spectrum for Bryn is shown. The falling weight exhibits a significant lower level at low frequencies below 10 Hz than the vibrations from the trains, but exceeds them above 15 Hz. The maximum vibration level for the train is around 5 Hz and around 90 dB for the position at 8 m and around 80 dB for the position at 12 m. The maximum level of the falling weight is around 65 dB at around 30 Hz. In figure 4.12 the spectrum in third octave bands is weighted. The maximum level of the train vibration is 85 dB at 5 Hz for the position of 8 m and 75 dB at 7 Hz for the position at 12 m, while the falling weight induces a vibration level of 55 dB at 15 Hz. The slightly higher level of the falling weight compared to the tram can be see above 20 Hz but is much lower than the maximum vibration level at 10 Hz and below.

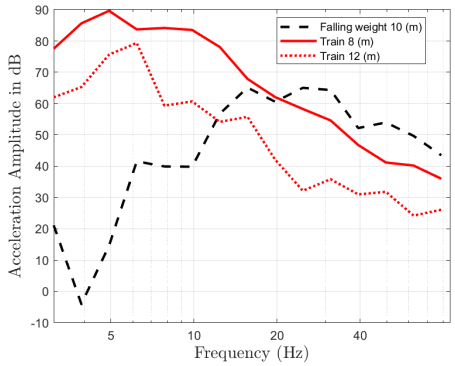


**Figure 4.11:** Frequency spectrum at Bryn in third octave bands.

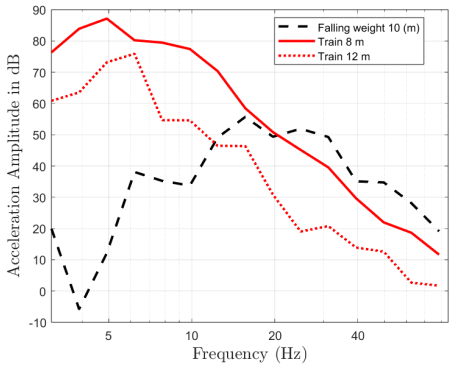


**Figure 4.12:** Weighted spectrum, third octave bands, Bryn.

In figure 4.13 the spectrum for Lyskåer is shown. The falling weight exhibits a significant lower level at low frequencies below 10 Hz than the vibrations from the trains, but exceeds them above 10 Hz. The maximum vibration level for the train is around 60 Hz and around 95 dB for the position at 8 m and around 60 dB for the position at 12 m. The maximum level of the falling weight is around 40 dB at around 40 Hz. In figure 4.14 the spectrum in third octave bands is weighted. The maximum level of the train vibration is 70 dB at 60 Hz for the position of 8 m and 45 dB at

5 Hz for the position at 12 m, while the falling weight induces a vibration level of 30 dB at 25 Hz. The trains had a clear peak at around 60 Hz. The falling weight had lower levels at most frequencies compared to the train. With the weighting for the train at 12 m the peak changed from 60 Hz to 5 Hz.

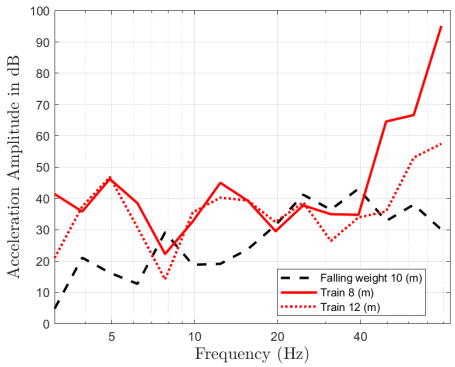


**Figure 4.13:** Frequency spectrum at Lysåker in third octave bands.

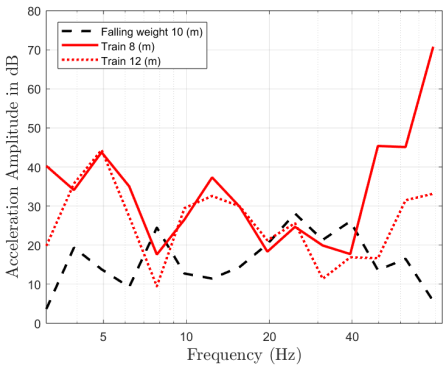


**Figure 4.14:** Weighted spectrum, third octave bands, Lysåker.

The background level for Nordstrand is also presented in figure 4.15 with no weighting applied. Below 3 Hz the background level is higher than the falling weight. At all other frequencies is the background significantly lower.

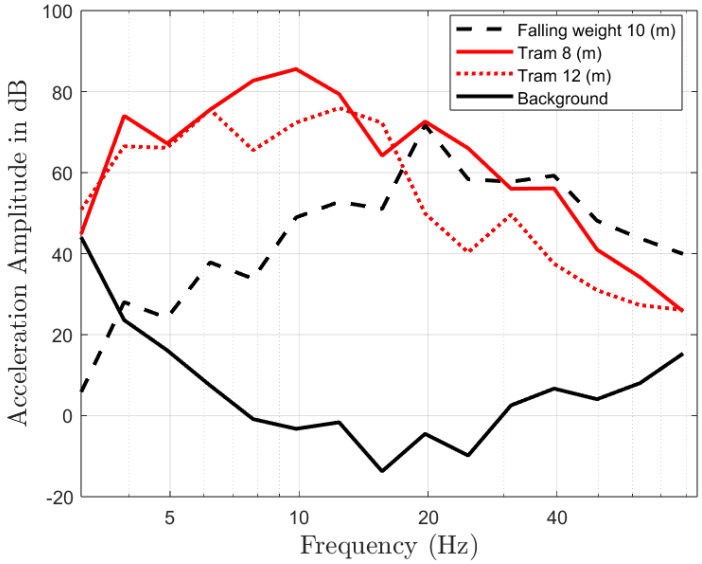


**Figure 4.15:** Frequency spectrum at Nordstrand in third octave bands with the background level

## 4.3 Linear regression of vibration decay

The linear regression of the decay is presented for each vehicle passing. The data for the linear regression is the max rms acceleration value. For the rail vehicles all the sensors are used as entry data. But for the falling weight the first sensor is ignored since the uncertainty of the distance between the sensor and the excitation is to large. The decay is given in reduction in level dB per doubling of the distance.

In table 4.1 the linear regression for the measurements in Grefsen is presented. The trams have a large range of decays from $-5.85\,\mathrm{dB}$ per doubling of the distance to $-9.79\,\mathrm{dB}$. The falling weight with the lowest energy had a lower decay at $-7\,\mathrm{dB}$ compared to the other two that had around $-8\,\mathrm{dB}$.

**Table 4.1:** Decay at Grefsen

| **Description** | **Value** |
|---|---|
| **Train** | |
| Train 1 | -7.33 |
| Train 2 | -8.26 |
| Train 3 | -5.85 |
| Train 4 | -7.30 |
| Train 5 | -9.79 |
| **Falling Weight** | |
| Falling Weight 50 | -7.00 |
| Falling Weight 80 | -8.09 |
| Falling Weight 100 | -8.00 |

In table 4.2 the linear regression for the measurements in Nordstrand is presented. The trams was consistent with half the vehicles having a decay around $-4.75\,\mathrm{dB}$ per doubling of the distance and the other half around $-6.5\,\mathrm{dB}$. The falling weight had a similar decay for all measurements at around $-7.4\,\mathrm{dB}$.

**Table 4.2:** Decay at Nordstrand

| Description | Value |
|---|---|
| **Train** | |
| Train 1 | -6.40 |
| Train 2 | -4.50 |
| Train 3 | -6.34 |
| Train 4 | -4.83 |
| Train 5 | -6.76 |
| Train 6 | -4.74 |
| Train 7 | -6.59 |
| Train 8 | -4.96 |
| **Falling Weight** | |
| Falling Weight 50 | -7.62 |
| Falling Weight 80 | -7.38 |
| Falling Weight 100 | -7.37 |

In table 4.3 the linear regression for the measurement in Bryn is presented. The trams have a medium range of decays from $-8.50\,\mathrm{dB}$ per doubling of the distance to $-11.34\,\mathrm{dB}$. The falling weight had a decay from $-6\,\mathrm{dB}$ to $-7\,\mathrm{dB}$ witch is lower then the decay from the trains.

**Table 4.3:** Decay at Bryn

| Description | Value |
|---|---|
| **Train** | |
| Train 1 | -9.93 |
| Train 2 | -11.34 |
| Train 3 | -8.50 |
| **Falling Weight** | |
| Falling Weight 50 | -6.06 |
| Falling Weight 80 | -6.30 |
| Falling Weight 100 | -7.04 |

In table 4.4 the linear regression for the measurements in Lysåker is presented. The trams have a large range of decays from $-3.23\,\mathrm{dB}$ per doubling of the distance to $-8.25\,\mathrm{dB}$. The falling weight was around $-6\,\mathrm{dB}$ for all measurements.

**Table 4.4:** Decay at Lysaker

| Description | Decay |
|---|---|
| **Train** | |
| Train 1 | -8.25 |
| Train 2 | -3.62 |
| Train 3 | -4.83 |
| Train 4 | -4.28 |
| Train 5 | -3.26 |
| Train 6 | -6.97 |
| Train 7 | -3.23 |
| Train 8 | -6.16 |
| **Falling Weight** | |
| Falling Weight 50 | -6.16 |
| Falling Weight 80 | -6.04 |
| Falling Weight 100 | -6.20 |

An average decay of the rail vehicles and the falling weight at each location was also calculated by doing a linear regression of the average energy at each distance. A comparison between the decay of all the measurements are presented in figure 4.16. At Grefsen the decay was similar for trams and the falling. At Bryn on the other hand a the two methods gave completely different results. At both Lysåker and Nordstrand the decay was slightly more for the rail vehicle.

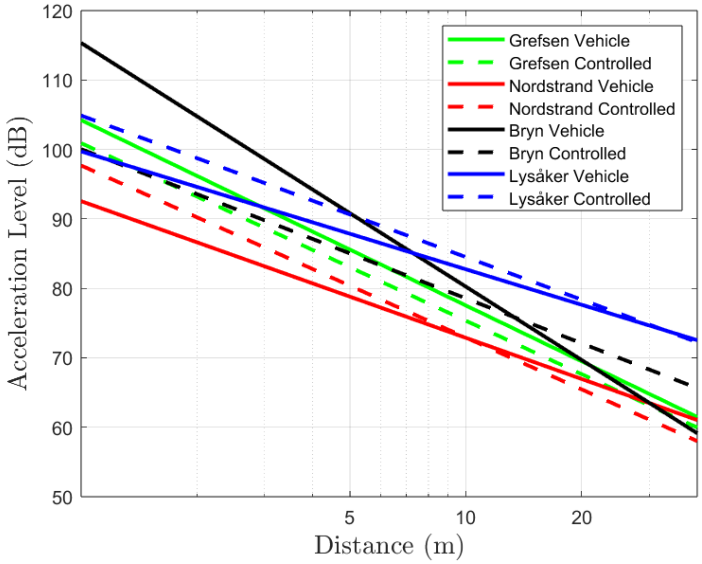


**Figure 4.16:** An average vibration decay for all trams/trains and falling weight at each location

## 4.4 Model for rail vehicle using controlled excitation

The last step investigates the decay of the measurements compared to theoretical geometrical attenuation. The theoretical attenuation for surface waves is calculated using equation (2.3). In table 4.2 it is concluded that the falling weight decays more rapid then the train. Considering this, a model of the tram representing as a finite line source is created.

In figure 4.17 the theoretical line- and point source decay is given as well as the model of representing the line source by adding theoretical point sources. In figure 4.18 the decay of a tram and the falling weight is presented as well as the same model but with the point sources being the decay from the falling weight.

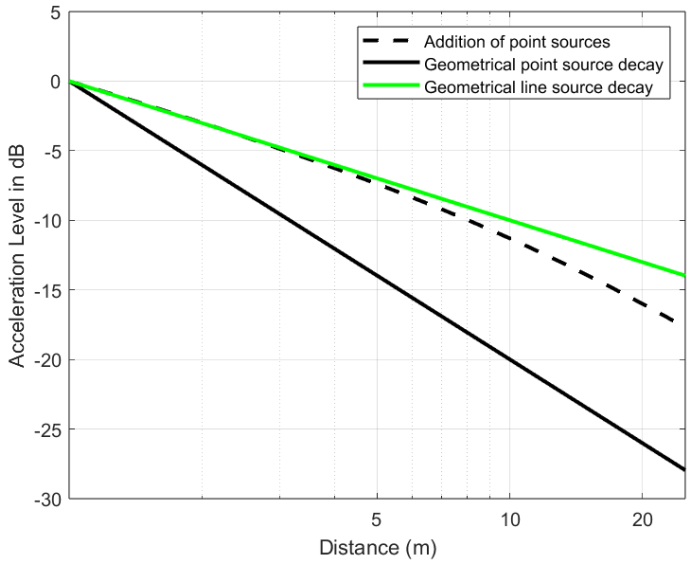


**Figure 4.17:** Regression model compared to the theoretical geometrical attenuation

In figure 4.17 the model behaves like a line source until around 7 meters when the attenuation starts increasing. At distances closer to 20 meters the model behave more like a point source than a line source. This model, based on the falling weight decay, is then used on a singular vehicle decay at Nordstrand. In figure 4.18 it shows how this model match well with the decay of the tram up until 20 meters. The last step is applying the model to all locations. This is then comparing to the average ground vibration decay from rail vehicles presented in figure 4.16. This comparison is presented in figure 4.19.

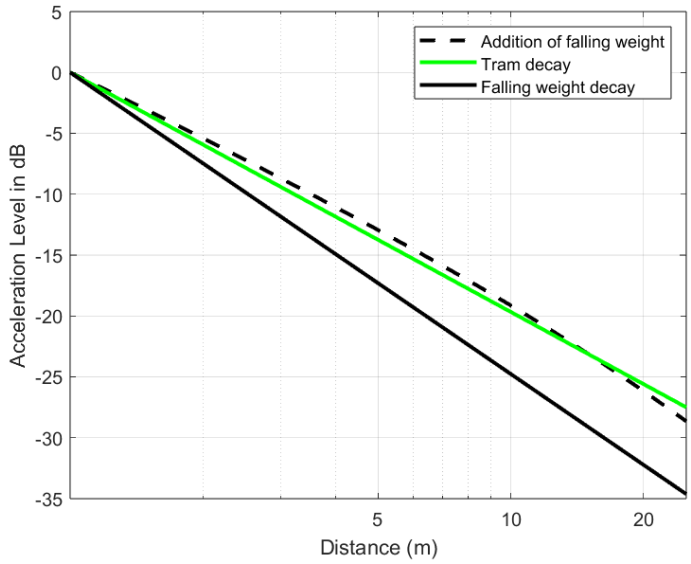


**Figure 4.18:** Regression model of a individual tram at Nordstrand

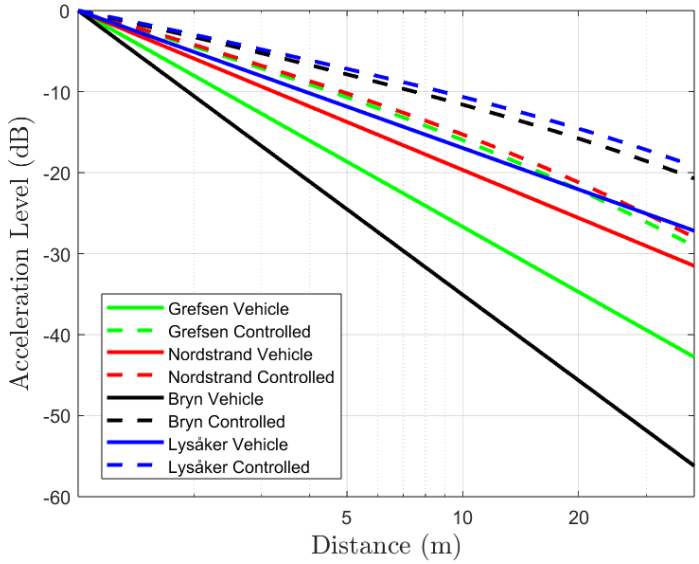


**Figure 4.19:** Regression model of all locations compared to the average rail vehicle regression

## 4.5 Numerical method

This section presents the numerical method explained in the methodology. The results are the acceleration level normalized to the input power up to 20 meter from the source. Study only cover the frequency range from 1 Hz to 30 Hz due to computational power requirements. No frequency weighting is applied to the results. The results of the acceleration level over these parameters for the two models are shown in figure 4.20 and 4.21.

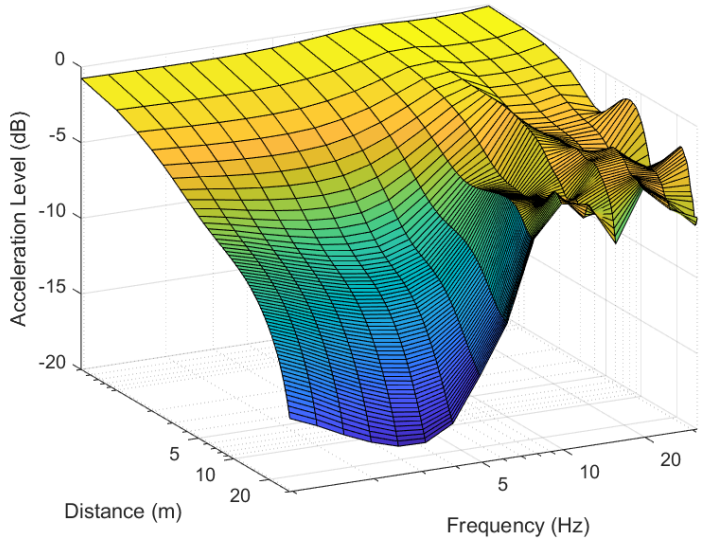


**Figure 4.20:** Numerical calculation, acceleration level in vertical direction, representing the ground conditions at Grefsen

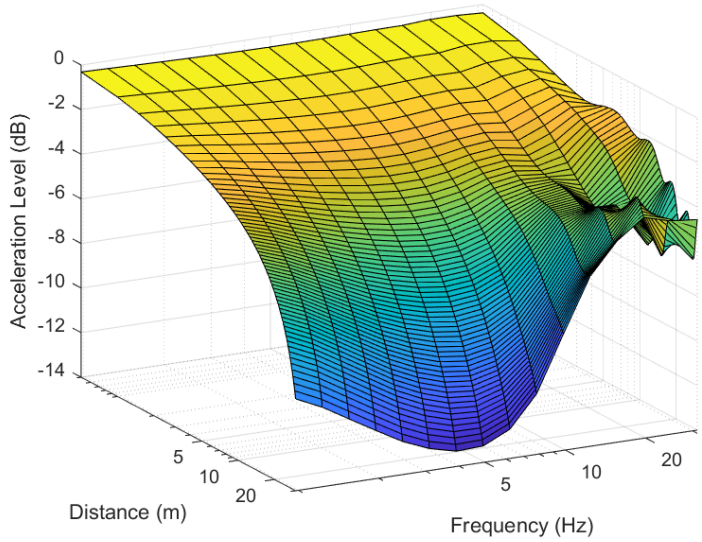


**Figure 4.21:** Numerical calculation, acceleration level in vertical direction, representing the ground conditions at Nordstrand

The decay of the of the lower frequencies is much lager in both the models. The model with a soil layer, see figure 4.20, have a wave pattern at around 10 Hz. A wave pattern, see figure 4.21 can also be observed in the model with only bedrock at around 20 Hz. The decay of ground vibrations is also compared in figure 4.22. Summing up and comparing both signals shows that is difference in decay at 20 meter is small. The largest discrepancies is that the vibration attenuate faster in the clay closer to the source. A bit further away, at over 5 meter from the source,

this wave pattern is observed and interpreted as reflections. Ground vibration from the model with only bedrock declines faster further from the source.

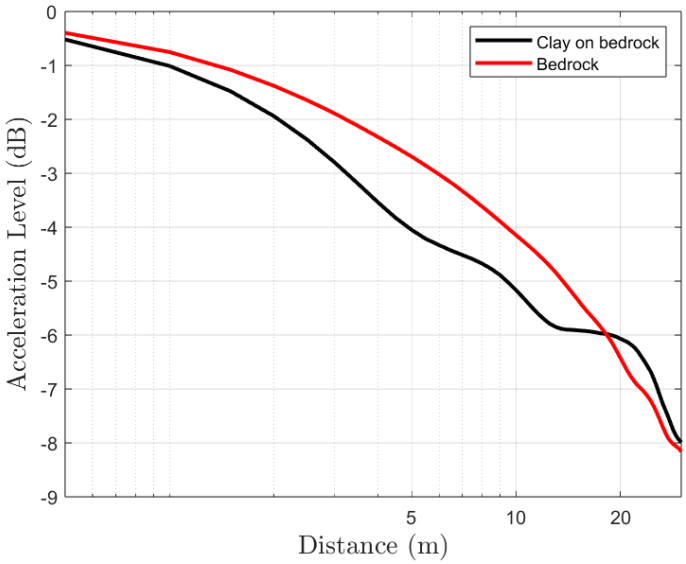


**Figure 4.22:** Compared decay with clay on top of bedrock compared to only bedrock.

# 5
# Discussion

## 5.1 Method discussion

This part of the discussion will be about the method used in this thesis. It will include problems and obstacles that occurred and solutions or other methods that could be used instead.

The method was an empirical method that used a falling weight to predict the ground vibrations from rail vehicles. The purpose was to create a scoping model that could be used at early stages in the planning process. While there have been some research on calculating transfer function using falling weights there is a lack of research using controlled sources to predict ground vibrations from rail vehicles. Other empirical, or semi empirical methods that are researched use rail vehicle measurements to tune different variables. Theses methods are presented in section 2.4.1 and rely on ground condition data. One advantage of the method used in this thesis is that there is not a need to only rely on previous ground condition data.

The method used faced some problems along the way. The equipment used when dropping the falling weight lacked consistency. Human error occurred when trying to release the weight from the same height each time and when trying to control the weight after impact. The ladder that the harness was mounted to was hard to place in the same position at different locations. The unevenness of the ground caused the ladder to sometimes tilt. That lead to further uncertainty at what height the weight was released from as well as problems with achieving a clean impact with the pad on the ground. The different environment at each location also caused the set up of the falling weight to be placed closer or further to the position of the first sensor. A possible error with the equipment occurred with the sensors and the set up of the sensors. More sensitive sensors like geophones would improve the accuracy of the measurement. The set up of the sensors also left room for errors in how they where mounted and connected to the ground and at what distance they where placed.

The method also had flaws regarding at what distance the sensor were from the track. The third sensor could be removed and placed at a distance between the first and the second sensor. This would make it more accurate when examining the influence of the near-field on the decay. The other problem regarding the distance was that two rail track was measured at each location. This caused the distance from the tracks to the sensor to not line up with the distance from the falling weight. A solution to this could be to two sensors placed, so that one have the exact same

distance from source to sensor for the track as for the falling weight. The method could also work better when planning new rail way. When planning a new rail way the falling weight could be dropped on the same location as the rail. This would mean that the same distance and the exact same ground conditions could be investigated.

Due to measuring rail vehicles in an urban area the number of locations available for the set up was limited. The locations that where picked also had specific properties. As an example at Bryn and Grefsen a paved walkway crossed the measurement set up. Also the topography of the locations presented a challenge with the sensors not being leveled. During the time of the measurement a tram line was under reconstruction. This forced the measurement of trams on bedrock to be moved to Nordstrand where the sensor furthest away had to be excluded to to environment restrictions.

The method used could be changed and improved in certain aspects. Due to problem with the amount of force input the weight should only be dropped at one, single fixed, height for all measurements. The distance dropped you be measured from the pad a each new location. There is a conflict in the method of how simple it should be contrary how accurate it should be. The current method only excite the ground at one point. Two alternative methods could be used here instead. Both would sill have identical set up of the sensors. The first alternative would have the falling weight source point moved along the railway. The other method would be to simultaneously drop multiple falling weights along the track. Both these would more accurately describe the ground conditions of the site. The second on could also potentially cover wave super position that can occur.

## 5.2 Result discussion

At some locations a large range of ground vibrations was observed. At both Grefsen and Lysåker the magnitude for measurements recorded at similar conditions gave drastically different acceleration levels. These locations both had a layer of soil on top of the bedrock. At the locations with only bedrock the acceleration levels did not vary as much for different vehicles. When comparing the two cases for speed dependency there seems to be no relationship regarding the vehicle speed and the acceleration level. This is most likely due to ground vibrations from rail vehicles are chaotic in nature and the results showed that similar conditions can give rise to a large spread of outcomes. When comparing the falling weight to the rail vehicles a pattern emerged. For bed rock a weight dropped at a higher height was best suited to estimate the rail vehicles. For soil on top of bedrock the weight dropped at the middle position seemed to fit better to the rail measurements. For the falling weigh there was not a consistency in acceleration levels. Locations with assumed similar ground conditions had a large difference 5 m from the source when the falling weight was dropped from the same height. At the measurement locations with bedrock a difference of 10 dB was observed.

Most of the energy in the ground vibrations from the rail vehicles where below 10 Hz. The ground vibrations from the falling weight had much more energy at higher levels, most with a peak at 20 Hz. The influence of this is even more transparent when comparing the weighted spectrum. The lower frequencies are weighed more important for human disturbance. The only outlier for the rail vehicle measurement is at Lysåker, were the peak in energy was at 60 Hz. But when comparing the weighed spectrum at this location it is observed that the difference in lower frequencies is still significant. In this thesis the same frequency weighting were applied to both the rail vehicle measurements and the falling weight measurements in alignment to ISO-Standard 8041. The result suggest that the frequency content of the to signals are different and that another weighting could be used for the falling weight. A problem is also presented when looking at the background level. For really low frequencies the falling weight measurement is concealed by the background noise. This indicates that the falling weight might be to light to properly excite the low frequencies.

The regression is compared to the theoretical geometrical attenuation of surface waves. Per doubling of the distance the decay is $-3$ dB for a line source and $-6$ dB for a point source. It is observed that some vehicles acted more as a line source and some as a point source. This is most likely due to some irregularity on one wheel causing a dynamic load that dominates the signal. These pass-by had the highest acceleration level and a similar decay to the falling weight. At Bryn the the regression for trains was substantially more than for the falling weights. Due to few measurements it is hard to predict the cause. It might have been caused by an ground conditions or equipment failure.

In the cases when single dynamic load dominated the signal the rail vehicles can be assumed to be a finite line source. The decay from the finite line source gradually increases the further from the source. When comparing to the tram measurements, addition of the falling weight decay seems to be a good estimate up until 20 m from the source. When comparing the model to the average decay it the relationship is poor. The model suggest that the decay is much less than what is measured in reality. At most locations the rail vehicle decay were better estimated by just the falling weight. Both the falling weight and the rail vehicles acted more as point sources.

The numerical model showed that there is a difference in ground conditions. A softer soil resulted in lower levels closer to the source. But at around 10 m from the source reflections from the underlying layer caused the decay to decrease. This model only presented solution from 1 Hz to 30 Hz. To compare the result with the measurement a model that have solutions up to 80 Hz would be necessary to compare the decay with weightings applied.

# 6
# Conclusion

This thesis aimed at developing a method to predict ground vibrations from rail vehicles. This was achieved by developing an empirical method of measuring both rail vehicle ground vibrations and using a controlled source for the same ground condition.

The method had some problems with being inconsistent with assuming similar ground conditions. There is uncertainty about the ground conditions because of limited soil data. The numerical model showed that a layer of soil on top of bedrock can create reflections. Improvements to the method of excitation and the equipment making the controlled excitation more consistent could be a solution. This may involve, for example, stabilizing the structure the weight is released from as well as leveling the ground under the pad. This would make the weight fall the same distance each time and achieve a better impact. Also, the relationship between the frequency spectrum of the rail vehicles and the falling weight was poor. A different frequency weighting for the falling weight could lead to a better estimation of the rail vehicle ground vibration. To properly excite the low frequencies, a heavier falling weight might be necessary. .

A model was also created that described the rail vehicles as finite line sources based on the controlled source excitation. The model prediction was good for some individual vehicles. But when comparing the average decay, the relationship between the measurements and the model did not show good agreement. The measurements rather indicated that both the rail vehicles and the controlled source had a similar decay that resembled a point source for surface waves.

## 6.1 Future work

Future work could investigate the frequency spectrum of the falling weight and develop a new frequency weighting. This could be combined with a new model. A model that assumes the decay of rail vehicle ground vibration to resemble the decay of a theoretical point source for surface waves. To expand on this thesis, a consideration of receiving structures could be included. This would mean measuring ground-borne noise with a study of a larger frequency range.

# Bibliography


[1] Tracey Navaei, Simon Blainey, John Preston, and William Powrie. Carbon footprinting of railway infrastructure: a standardized, consistent data collection method. *Carbon Management*, 15, 06 2024.

[2] E. Öhrström. Effects of exposure to railway noise—a comparison between areas with and without vibration. *Journal of Sound and Vibration*, 205(4):555–560, 1997.

[3] Andreas Seidler, Melanie Schubert, Yasmin Mehrjerdian, Klaus Krapf, Christian Popp, Irene van Kamp, Mikael Ögren, and Janice Hegewald. Health effects of railway-induced vibration combined with railway noise – a systematic review with exposure-effect curves. *Environmental Research*, 233:116480, 2023.

[4] Mechanical vibration — Ground-borne noise and vibration arising from rail systems Part 1: General guidance. Standard, International Organization for Standardization, Geneva, CH, March 2005.

[5] Roger Holmberg et al. Vibrations generated by traffic and building construction activities. Technical report, 1984.

[6] Daniel Ainalis, Loïc Ducarne, Olivier Kaufmann, Jean-Pierre Tshibangu, Olivier Verlinden, and Georges Kouroussis. Improved analysis of ground vibrations produced by man-made sources. *Science of The Total Environment*, 616-617:517–530, 2018.

[7] G. Holm, B. Andreasson, P. Bengtsson, A. Bodare, and H. Eriksson. Mitigation of track andground vibrations byhigh speed trains at ledsgard, sweden. *Swedish Deep Stabilization Research Centre*, 2002.

[8] David Thompson. Chapter 5 - wheel/rail interaction and excitation by roughness. In David Thompson, editor, *Railway Noise and Vibration*, pages 127–173. Elsevier, Oxford, 2009.

[9] T. Fujikake. A prediction method for the propagation of ground vibration from railway trains. *Journal of Sound and Vibration*, 111(2):357–360, 1986.

[10] Victor V. Krylov and Colin C. Ferguson. Calculation of low-frequency ground vibrations from railway trains. 1 1994.

[11] Mario Bačić, Lovorka Librić, Danijela Jurić Kaćunić, and Meho Saša Kovačević. The usefulness of seismic surveys for geotechnical engineering in karst: Some practical examples. *Geosciences*, 10(10):406, 2020. Distributed under CC BY 4.0.

[12] Steven Earle. *Physical Geology*. BCcampus, Victoria, B.C., 2015. Distributed under CC BY 4.0.

[13] LukeTriton. Rayleigh and love waves, 2023. CC BY-SA 4.0, `https://commons.wikimedia.org/w/index.php?curid=133937782`.

[14] M. Heckl, G. Hauck, and R. Wettschureck. STRUCTURE-BORNE SOUND AND VIBRATION FROM RAIL TRAFFIC. *Journal of Sound and Vibration*, 193(1):175–184, 1996.

[15] David Thompson. Chapter 12 - low frequency ground vibration. In David Thompson, editor, *Railway Noise and Vibration*, pages 399–435. Elsevier, Oxford, 2009.

[16] Lars Hall, Carl Wersäll, K. Rainer Massarsch, and Anders Bodare. *SGF Informationskrift 1:2012: Markvibrationer*. 12 2015.

[17] Dong-Soo Kim and Jin-Sun Lee. Propagation and attenuation characteristics of various ground vibrations. *Soil Dynamics and Earthquake Engineering*, 19(2):115–126, 2000.

[18] Guangyun Gao, Jian Song, and Jun Yang. Identifying boundary between near field and far field in ground vibration caused by surface loading. *Journal of Central South University*, 21:3284–3294, 08 2014.

[19] Horace Lamb. I. on the propagation of tremors over the surface of an elastic solid. *Philosophical Transactions of the Royal Society of London. Series A, Containing Papers of a Mathematical or Physical Character*, 203:1–42, 1904.

[20] M. Bahrekazemi. *Train-Induced Ground Vibration and Its Prediction*. Phd dissertation, Byggvetenskap, 2004.

[21] C. Madshus, B. Bessason, and L. Hårvik. Prediction model for low frequency vibration from high speed railways on soft ground. *Journal of Sound and Vibration*, 193(1):195–203, 1996.

[22] G. Kouroussis, L. Van Parys, C. Conti, and O. Verlinden. Using three-dimensional finite element analysis in time domain to model railway-induced ground vibrations. *Advances in Engineering Software*, 70:63–76, 2014.

[23] X. Sheng, C.J.C. Jones, and David Thompson. Prediction of ground vibration from trains using the wavenumber finite and boundary element methods. *Journal of Sound and Vibration*, 293:575–586, 06 2006.

[24] S. L. Grassie, R. W. Gregory, D. Harrison, and K. L. Johnson. The dynamic response of railway track to high frequency vertical excitation. *Journal of Mechanical Engineering Science*, 24(2):77–90, June 1982.

[25] Vibrasjoner og støt - måling i bygninger av vibrasjoner fra landbasert samferdsel, vibrasjonsklasser og veiledning for bedømmelse av virkning på mennesker. *SN*, 2017.

[26] NGU. Borehull - dyp til fjell - med løsmassegeologi, 2024.

[27] NGU. Løsmasser, 2024.

[28] Buller och vibrationer från spårburen linjetrafik. Technical report, Banverket, 1997.

[29] Human response to vibration – measuring instrumentation –part 1: General purpose vibration meters (. Technical report, International Organization for Standardization, 2017.

# A

# Appendix 1

**Table A.1:** Factor and Center Frequency Table

| **Factor** | Center Frequency (Hz) |
|---|---|
| **0.8329** | 1 |
| **0.9071** | 1.25 |
| **0.9342** | 1.6 |
| **0.9319** | 2 |
| **0.9101** | 2.5 |
| **0.8721** | 3.15 |
| **0.8184** | 4 |
| **0.7498** | 5 |
| **0.6692** | 6.3 |
| **0.5819** | 8 |
| **0.4941** | 10 |
| **0.4114** | 12.5 |
| **0.3375** | 16 |
| **0.2738** | 20 |
| **0.2203** | 25 |
| **0.1760** | 31.5 |
| **0.1396** | 40 |
| **0.1093** | 50 |
| **0.08336** | 63 |
| **0.06036** | 80 |

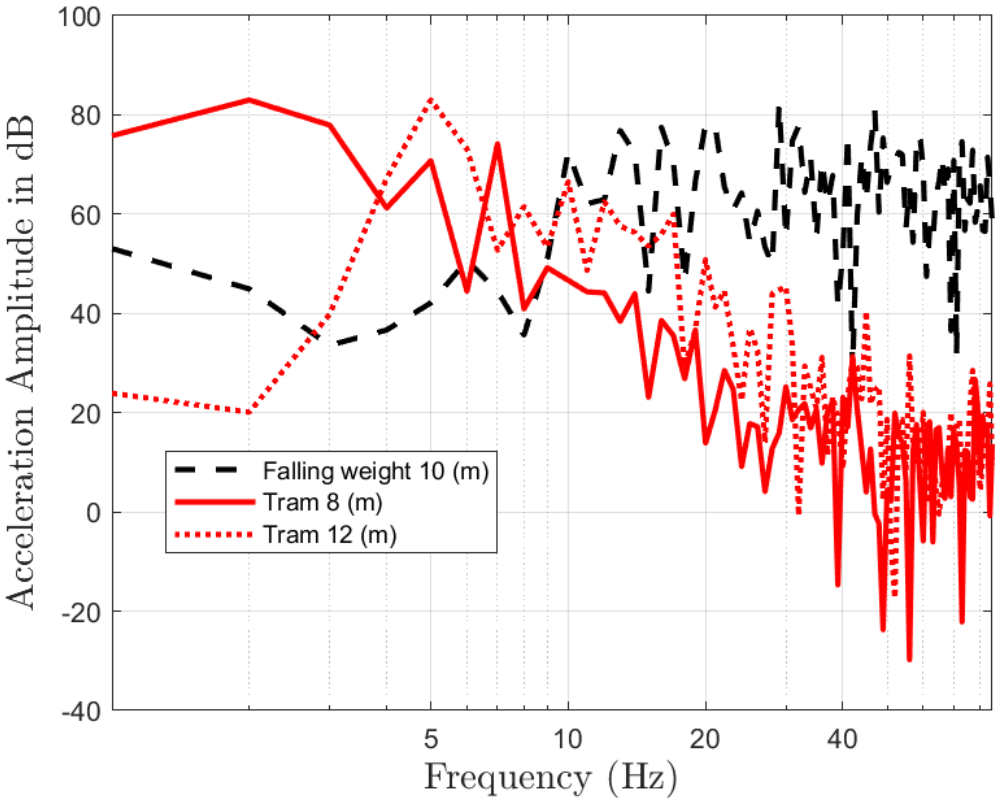


**Figure A.1:** Frequency spectrum at Grefsen in narrow bands

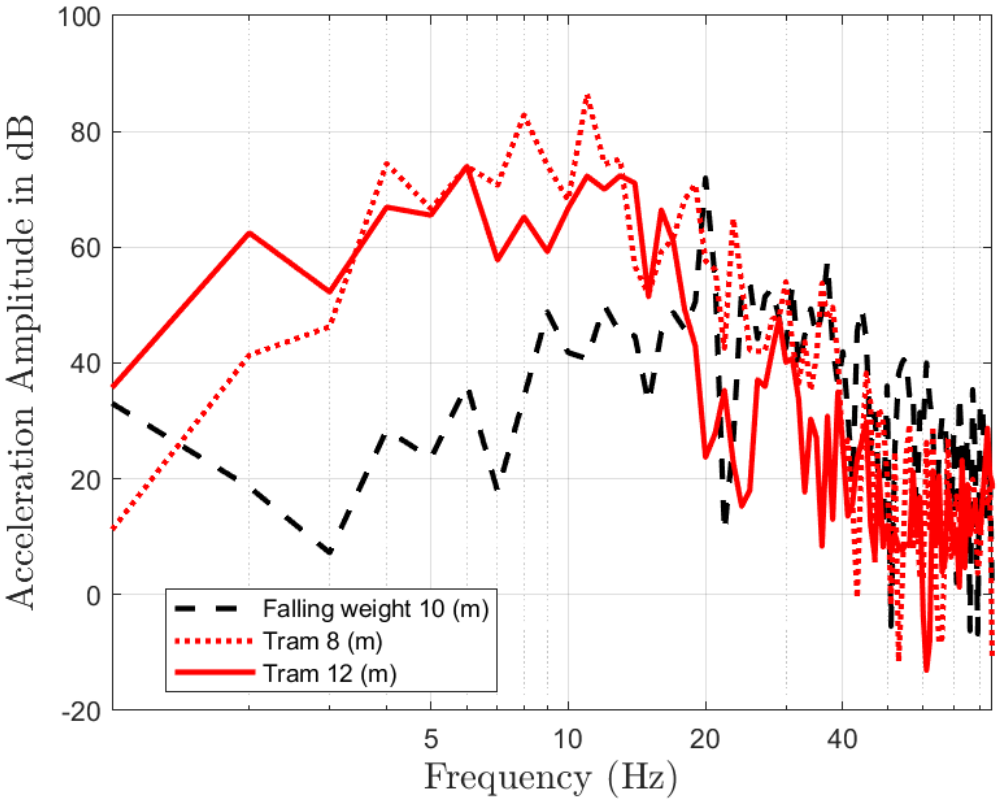


**Figure A.2:** Frequency spectrum at Nordstrand in narrow bands

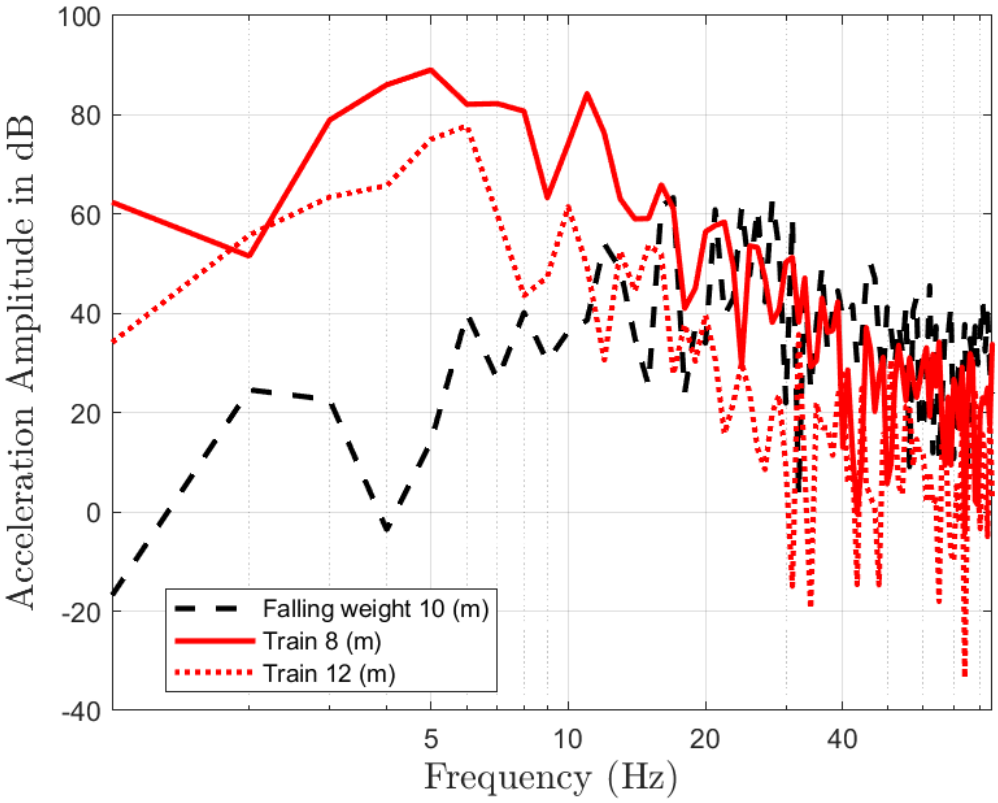


**Figure A.3:** Frequency spectrum at Bryn in narrow band

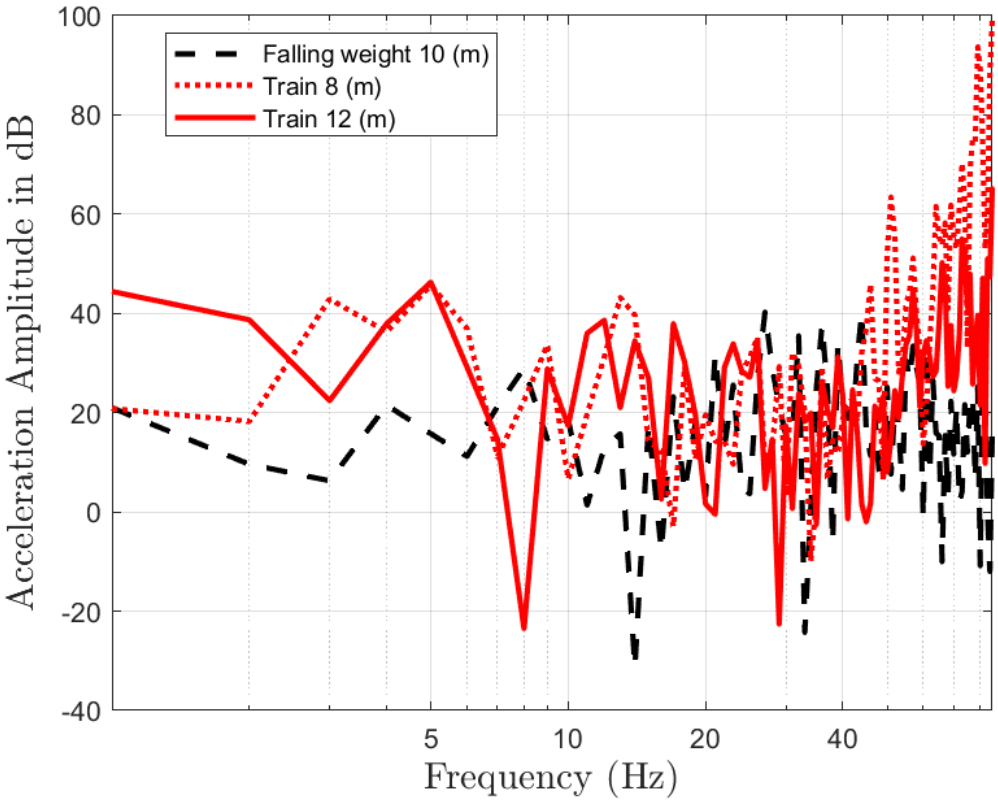


**Figure A.4:** Frequency spectrum at Lysåker in narrow band

**DEPARTMENT OF SOME SUBJECT OR TECHNOLOGY**
**CHALMERS UNIVERSITY OF TECHNOLOGY**
Gothenburg, Sweden
www.chalmers.se


CHALMERS
UNIVERSITY OF TECHNOLOGY